

Supporting Information

Tuning the Defect of Triple Conducting Oxide $\text{BaCo}_{0.4}\text{Fe}_{0.4}\text{Zr}_{0.1}\text{Y}_{0.1}\text{O}_{3-\delta}$
Perovskite Toward Activity Enhanced Cathode of Protonic Ceramic Fuel Cells

Rongzheng Ren,^a Zhenhua Wang,^{,a,b} Chunming Xu,^a Wang Sun,^{a,b} Jinshuo Qiao,^a David W.
Rooney^c and Kening Sun^{*,a,b}*

^a Beijing Key Laboratory for Chemical Power Source and Green Catalysis, School of Chemistry and Chemical Engineering, Beijing Institute of Technology, Beijing, 100081, People's Republic of China.

^b Collaborative Innovation Center of Electric Vehicles in Beijing, No.5 Zhongguancun South Avenue, Haidian District, Beijing, 100081, People's Republic of China

^c School of Chemistry and Chemical Engineering, Queen's University, Belfast, Northern Ireland BT9 5AG, United Kingdom

Corresponding Author

*Email: bitkeningsun@163.com (Kening Sun); wangzh@bit.edu.cn (Zhenhua Wang).

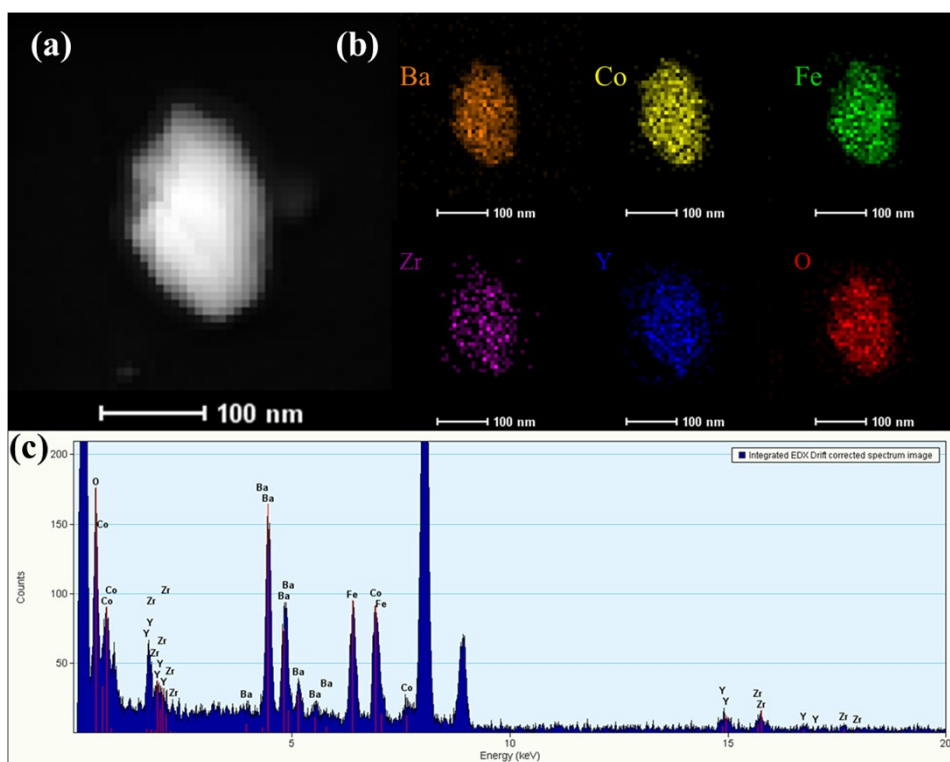


Fig. S1 Typical STEM image (a); EDS elemental distributions (b) and corresponding EDS results in the $\text{Ba}_{0.9}\text{Co}_{0.4}\text{Fe}_{0.4}\text{Zr}_{0.1}\text{Y}_{0.1}\text{O}_{3-\delta}$ oxide.

Table S1. The atomic percentage of each metal elements in $\text{Ba}_{0.9}\text{Co}_{0.4}\text{Fe}_{0.4}\text{Zr}_{0.1}\text{Y}_{0.1}\text{O}_{3-\delta}$ sample estimated by STEM-EDS analysis.

Elements		Ba	Co	Fe	Zr	Y
Atomic percentage (%)	Set	47.37 ($\frac{0.9}{1.9}$)	21.05 ($\frac{0.4}{1.9}$)	21.05 ($\frac{0.4}{1.9}$)	5.26 ($\frac{0.1}{1.9}$)	5.26 ($\frac{0.1}{1.9}$)
	Test	47.45	21.12	21.18	5.14	5.11

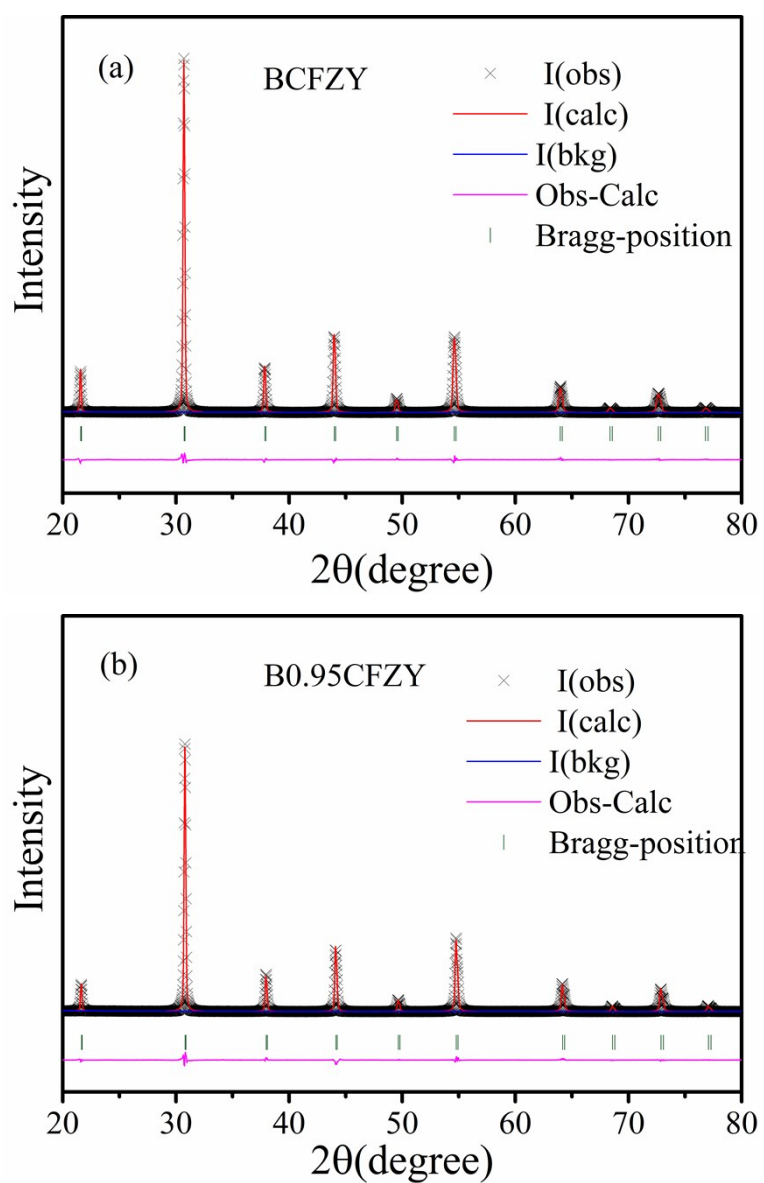


Fig.S2 Room temperature powder XRD patterns with Rietveld refinements results of (a)

$\text{BaCo}_{0.4}\text{Fe}_{0.4}\text{Zr}_{0.1}\text{Y}_{0.1}\text{O}_{3-\delta}$ and (b) $\text{Ba}_{0.95}\text{Co}_{0.4}\text{Fe}_{0.4}\text{Zr}_{0.1}\text{Y}_{0.1}\text{O}_{3-\delta}$.

Table S2. Summary of Rietveld refinement results of powder X ray diffraction for $\text{Ba}_x\text{Co}_{0.4}\text{Fe}_{0.4}\text{Zr}_{0.1}\text{Y}_{0.1}\text{O}_{3-\delta}$ ($x=1, 0.95, 0.9$)

Samples	$\text{BaCo}_{0.4}\text{Fe}_{0.4}\text{Zr}_{0.1}\text{Y}_{0.1}\text{O}_{3-\delta}$	$\text{Ba}_{0.95}\text{Co}_{0.4}\text{Fe}_{0.4}\text{Zr}_{0.1}\text{Y}_{0.1}\text{O}_{3-\delta}$	$\text{Ba}_{0.9}\text{Co}_{0.4}\text{Fe}_{0.4}\text{Zr}_{0.1}\text{Y}_{0.1}\text{O}_{3-\delta}$
Space group	Pm -3m	Pm -3m	Pm -3m
Cell parameters	a=b=c=4.112(8) $\alpha=\beta=\gamma=90^\circ$ density=5.866 g·cm ⁻³	a=b=c=4.101(0) $\alpha=\beta=\gamma=90^\circ$ density=5.718 g·cm ⁻³	a=b=c=4.093(3) $\alpha=\beta=\gamma=90^\circ$ density=5.544 g·cm ⁻³
Ba, 1b, 0, 0, 0			
Uiso, Occupancy	0.00137, 1	0.00284, 0.95	0.00182, 0.9
Co, 1a, 1/2, 1/2, 1/2			
Uiso, Occupancy	0.01682, 0.4	0.05033, 0.4	0.05266, 0.4
Fe, 1a, 1/2, 1/2, 1/2			
Uiso, Occupancy	0.00034, 0.4	0.00036, 0.4	0.000492, 0.4
Zr, 1a, 1/2, 1/2, 1/2			
Uiso, Occupancy	0.0003, 0.1	0.00479, 0.1	0.00195, 0.1
Y, 1a, 1/2, 1/2, 1/2			
Uiso, Occupancy	0.00011, 0.1	0.00178, 0.1	0.01167, 0.1
O, 3d, 1/2, 0, 1/2			
Uiso, Occupancy	0.03782, 0.9274	0.04371, 0.8982	0.03187, 0.8637
Riveted Refinement	$R_p=3.76\%$	$R_p=4.37\%$	$R_p=3.65\%$
Parameters	$R_{wp}=5.07\%$	$R_{wp}=5.65\%$	$R_{wp}=5.25\%$
	$\chi^2=2.338$	$\chi^2=2.203$	$\chi^2=1.966$

Table S3. The composition of lattice oxygen and surface adsorption oxygen species in $\text{Ba}_x\text{Co}_{0.4}\text{Fe}_{0.4}\text{Zr}_{0.1}\text{Y}_{0.1}\text{O}_{3-\delta}$ ($x=1, 0.95, 0.9$) oxides obtained from fitting peaks.

Samples	$\text{O}_{\text{lattice}}$			O_{abs}			Area ratio
	Position (eV)	Area	FWHM (eV)	Position (eV)	Area	FWHM (eV)	$\text{O}_{\text{lattice}}/\text{O}_{\text{abs}}$
$x=1.00$	528.196	12336	1.047	530.762	21698	1.677	0.568
$x=0.95$	528.124	7154	1.004	530.773	22515	2.016	0.317
$x=0.90$	528.147	4722	1.187	530.727	17907	1.748	0.264

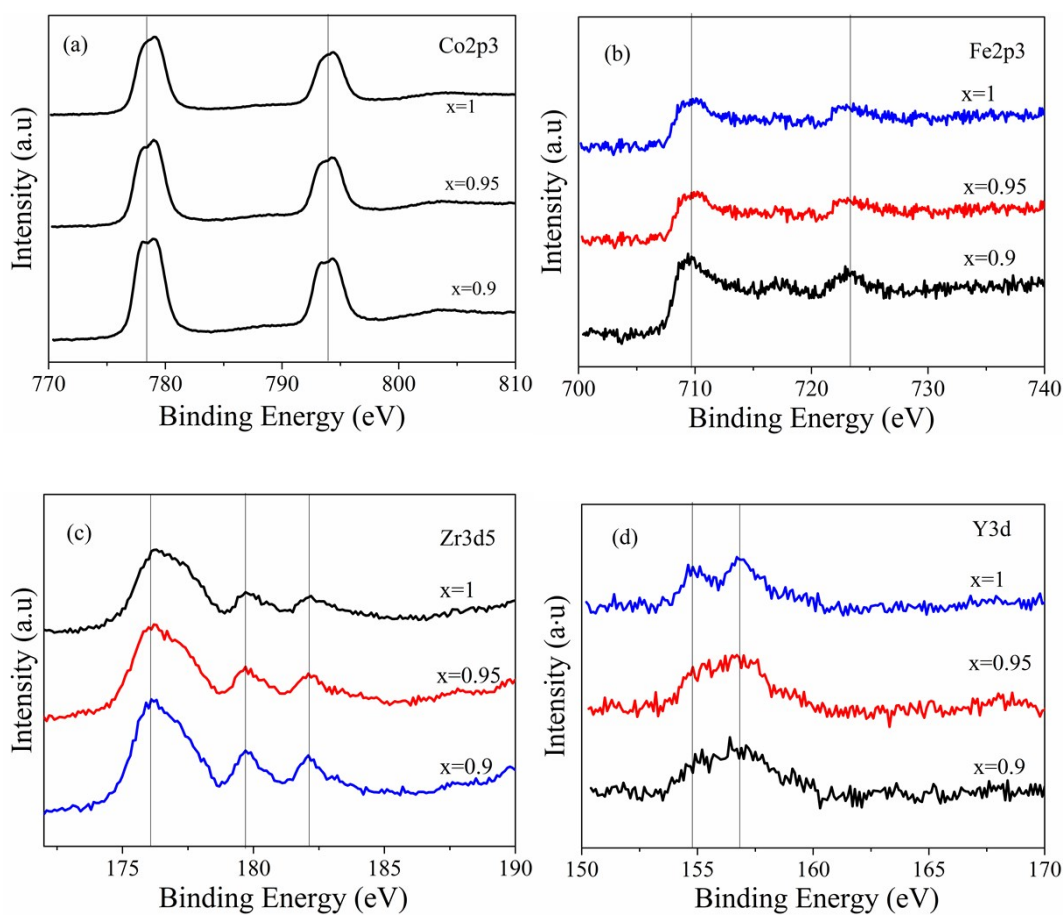
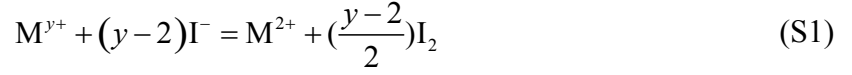


Fig. S3 XPS spectra of $\text{Ba}_x\text{Co}_{0.4}\text{Fe}_{0.4}\text{Zr}_{0.1}\text{Y}_{0.1}\text{O}_{3-\delta}$ ($x=1, 0.95, 0.9$) powders: (a) Co 2p, (b) Fe 2p, (c) Zr 3d, and (d) Y 3d.

In $\text{Ba}_x\text{Co}_{0.4}\text{Fe}_{0.4}\text{Zr}_{0.1}\text{Y}_{0.1}\text{O}_{3-\delta}$ ($x = 1, 0.95, 0.9$) system, only Co and Fe ions show variable valence and can be reduced by I^- ions. So the oxygen nonstoichiometry (δ) can be determined by the iodometry titration method. The chemical eqs involved in titration process are listed in eq S1 and S2.



Where M represents Co and Fe elements, and y is their average valence state.

Based on the mass conservation during the chemical reaction, the eq S3 can be obtained.

$$\frac{0.8m}{xM_{\text{Ba}} + 0.4M_{\text{Fe}} + 0.4M_{\text{Co}} + 0.1M_{\text{Zr}} + 0.1M_{\text{Y}} + (3-\delta)M_{\text{O}}} = (y-2)cV \quad (\text{S3})$$

Where m is the mass of samples, M is the molar mass of the corresponding element, c and V denotes the concentration and volume of $\text{Na}_2\text{S}_2\text{O}_3$ standard solution, respectively.

According to the charge neutrality in $\text{Ba}_x\text{Co}_{0.4}\text{Fe}_{0.4}\text{Zr}_{0.1}\text{Y}_{0.1}\text{O}_{3-\delta}$ ($x = 1, 0.95, 0.9$) system, the eq S4 can also be obtained.

$$2x + 0.8y + 4 \times 0.1 + 3 \times 0.1 = 2(3-\delta) \quad (\text{S4})$$

Obviously, oxygen vacancy content of the sample and the average oxidation states of Co/Fe ions can be calculated by solving the roots of eq S3 and S4. And the results were listed in Table S3.

Table S4. Oxygen nonstoichiometry (δ) in $\text{Ba}_x\text{Co}_{0.4}\text{Fe}_{0.4}\text{Zr}_{0.1}\text{Y}_{0.1}\text{O}_{3-\delta}$ ($x=1, 0.95, 0.9$) oxides at room temperature measured by the iodometry titration method.

Samples	Mass of sample (g)	Volume of $\text{Na}_2\text{S}_2\text{O}_3$ solution* (mL)	δ	Average valence of Co/Fe ions
x = 1	0.0318	14.66	0.29	3.41
x = 0.95	0.0302	14.58	0.33	3.43
x = 0.9	0.0312	15.98	0.36	3.47

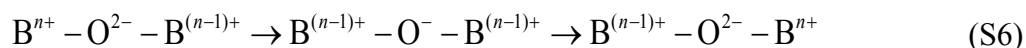
*The concentration of $\text{Na}_2\text{S}_2\text{O}_3$ standard solution is calibrated to $0.011 \text{ mol}\cdot\text{L}^{-1}$.

The oxygen nonstoichiometry at the high temperatures (δ_t) was calculated using eq S5 based on the TG test of samples in air.

$$\delta_t = \delta_0 + \frac{(m_0 - m_t) \times (M - 15.9994\delta_0)}{15.9994m_0} \quad (\text{S5})$$

where m_0 is the initial and m_t means the actual weight of the $\text{Ba}_x\text{Co}_{0.4}\text{Fe}_{0.4}\text{Zr}_{0.1}\text{Y}_{0.1}\text{O}_{3-\delta}$ sample at the interrelated temperature, while M means the molar mass of $\text{Ba}_x\text{Co}_{0.4}\text{Fe}_{0.4}\text{Zr}_{0.1}\text{Y}_{0.1}\text{O}_{3-\delta}$ with stoichiometric oxygen content.

The hopping transport mechanism of hole(electron) in ABO_3 perovskite can be ascribed to the Zener double exchange conduction process, where B^{n+} cation captures an electron from an adjacent $B^{(n-1)+}$ cation mediated by the O 2p orbital as described in eq S6.¹



As shown in Figure S4, the electronic conductivity of B_xCFZY decreases with the increase of Ba deficiency. The main reason is probably that the appearance of oxygen vacancies ($B - V_O^{\ominus} - B$) interrupts the -B-O-B- links and thus impairs the Zener double exchange conduction process, leading to the decrease of electrical conductivity.²

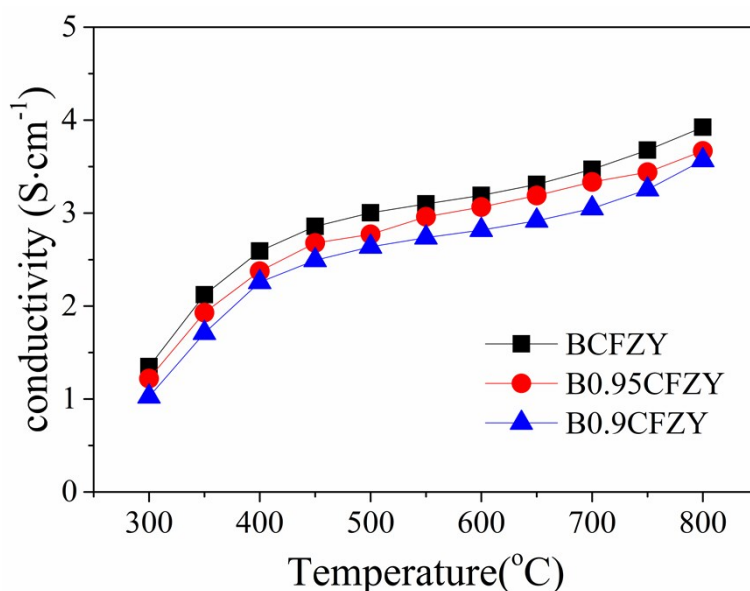


Fig. S4 Electrical conductivity of $Ba_xCo_{0.4}Fe_{0.4}Zr_{0.1}Y_{0.1}O_{3-\delta}$ ($x = 1, 0.95, 0.9$) oxides as a function of temperature measured at dry air.

The electrical conductivity relaxation (ECR) technique was employed using the testing apparatus shown in Figure S5(a).

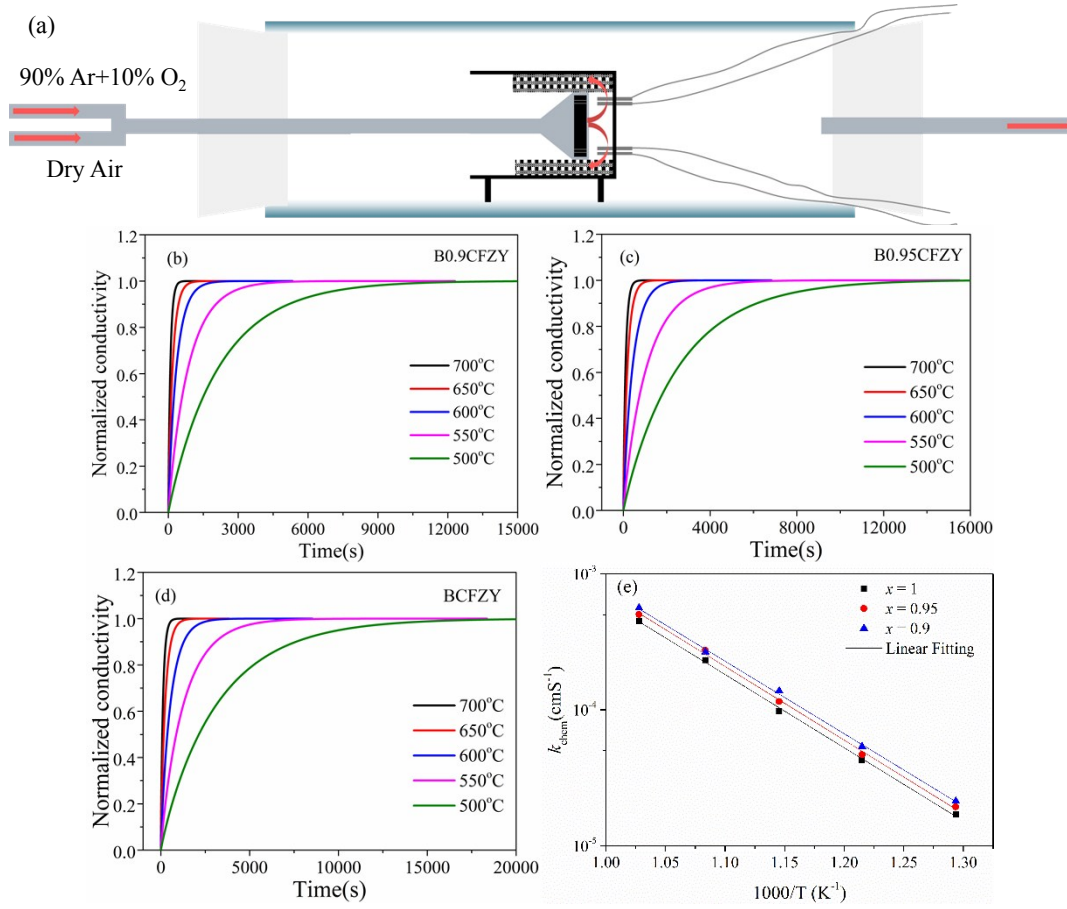


Fig. S5 Test and calculation of the electrical conductivity relaxation. (a) testing apparatus of ECR. And the ECR curves of (b) B0.9CFZY, (c) B0.95CFZY and (d) BCFZY at 500~700 °C after sudden change of oxygen partial pressure from 0.21 to 0.1 atm; (e) Temperature-dependence of fitted k_{chem} from 500 to 700 °C.

The chemical bulk diffusion coefficient (D_{chem}) and surface exchange coefficient (k_{chem}) were gotten by fitting the electrical conductivity relaxation curves with eq (S7).

$$f(t) = \frac{\sigma(t) - \sigma(0)}{\sigma(\infty) - \sigma(0)} = 1 - \sum_{m=1}^{\infty} \sum_{n=1}^{\infty} \sum_{l=1}^{\infty} \frac{2L_x^2 \exp\left(\frac{-\alpha_m^2 D_{\text{chem}} t}{x^2}\right)}{\alpha_m^2 (\alpha_m^2 + L_x^2 + L_x)} \times \frac{2L_y^2 \exp\left(\frac{-\beta_n^2 D_{\text{chem}} t}{y^2}\right)}{\beta_n^2 (\beta_n^2 + L_y^2 + L_y)} \times \frac{2L_z^2 \exp\left(\frac{-\gamma_l^2 D_{\text{chem}} t}{z^2}\right)}{\gamma_l^2 (\gamma_l^2 + L_z^2 + L_z)} \quad (\text{S7})$$

Where $f(t)$ is defined as normalized conductivity, while $\sigma(0)$, $\sigma(t)$ and $\sigma(\infty)$ denotes the initial, time dependent and final conductivity, respectively. And eq (S8) shows the calculation process of parameters L_x , L_y and L_z , respectively.

$$L_x = x \frac{k_{chem}}{D_{chem}}, L_y = y \frac{k_{chem}}{D_{chem}}, L_z = z \frac{k_{chem}}{D_{chem}} \quad (S8)$$

And the coefficient α_m , β_n and γ_l is the m -th, n -th and l -th positive root of the transcendental eq (S9), respectively.

$$\alpha_m \tan \alpha_m = L_x, \beta_n \tan \beta_n = L_y, \gamma_l \tan \gamma_l = L_z \quad (S9)$$

Table S5. k_{chem} and D_{chem} at various temperature for $Ba_xCo_{0.4}Fe_{0.4}Zr_{0.1}Y_{0.1}O_{3-\delta}$ ($x=1, 0.95, 0.9$) cuboid strip.

Temperature (°C)	$x = 0.9$		$x = 0.95$		$x = 1$	
	$k_{chem} \times 10^4$ ($cm \cdot s^{-1}$)	$D_{chem} \times 10^5$ ($cm^2 \cdot s^{-1}$)	$k_{chem} \times 10^4$ ($cm \cdot s^{-1}$)	$D_{chem} \times 10^5$ ($cm^2 \cdot s^{-1}$)	$k_{chem} \times 10^4$ ($cm \cdot s^{-1}$)	$D_{chem} \times 10^5$ ($cm^2 \cdot s^{-1}$)
700	5.62	4.50	5.03	3.14	4.51	2.38
650	2.67	2.08	2.74	1.59	2.32	1.04
600	1.38	1.14	1.15	0.85	0.97	0.55
550	0.54	0.57	0.47	0.29	0.43	0.21
500	0.213	0.22	0.19	0.13	0.17	0.085

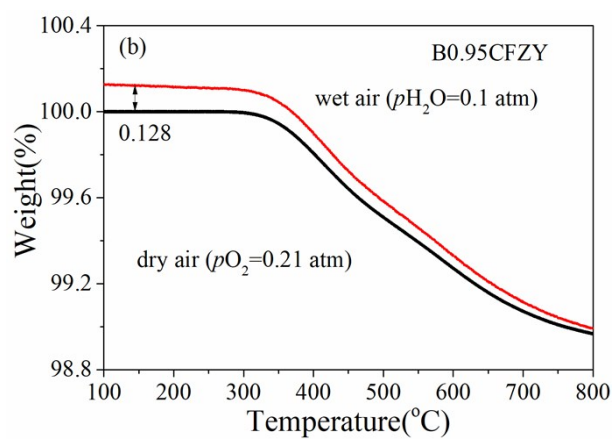
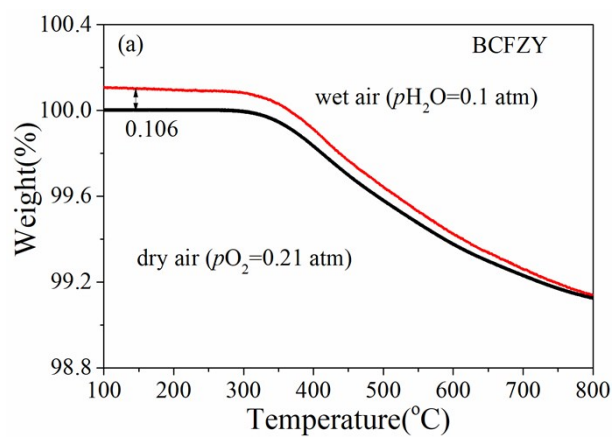


Fig. S6. Thermogravimetric curves of (a) BCFZY and (b) B0.95CFZY during cooling stage under dry and wet air.

The formation of proton is through the combination of water and oxygen vacancies in cathode materials. And the water is also produced in the cathode of PCFCs. So a good chemical compatibility is very necessary between B_xCFZY materials and water. To check it, hydrated materials were prepared with the following procedure. The raw B_xCFZY powders were annealed under wet air ($p_{\text{H}_2\text{O}} = 1 \text{ atm}$, extreme wet condition to ensure the reliability) from 800 °C down to 500 °C with a cooling rate of 5 °C/min, followed by a temperature platform of 500 °C for 10 h, an enough duration to ensure the combination of water and oxygen vacancies. The sample was then cooled down slowly (5 °C/min) to the room temperature. The hydrated B_xCFZY materials were tested by XRD to check the possible phase transition as shown in Figure S6.

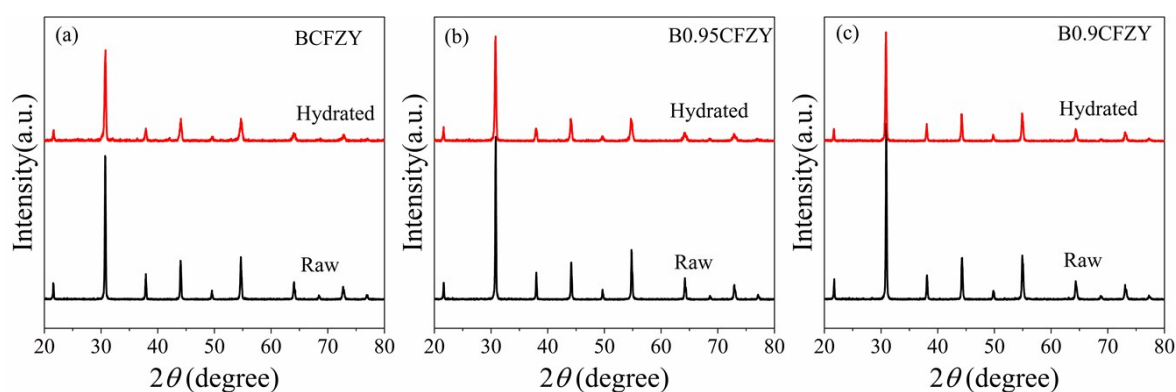


Fig. S7. XRD patterns of raw and hydrated $\text{Ba}_x\text{Co}_{0.4}\text{Fe}_{0.4}\text{Zr}_{0.1}\text{Y}_{0.1}\text{O}_{3-\delta}$ ($x = 1, 0.95, 0.9$) oxides.

(a) $x = 1$, (b) $x = 0.95$, (c) $x = 0.9$.

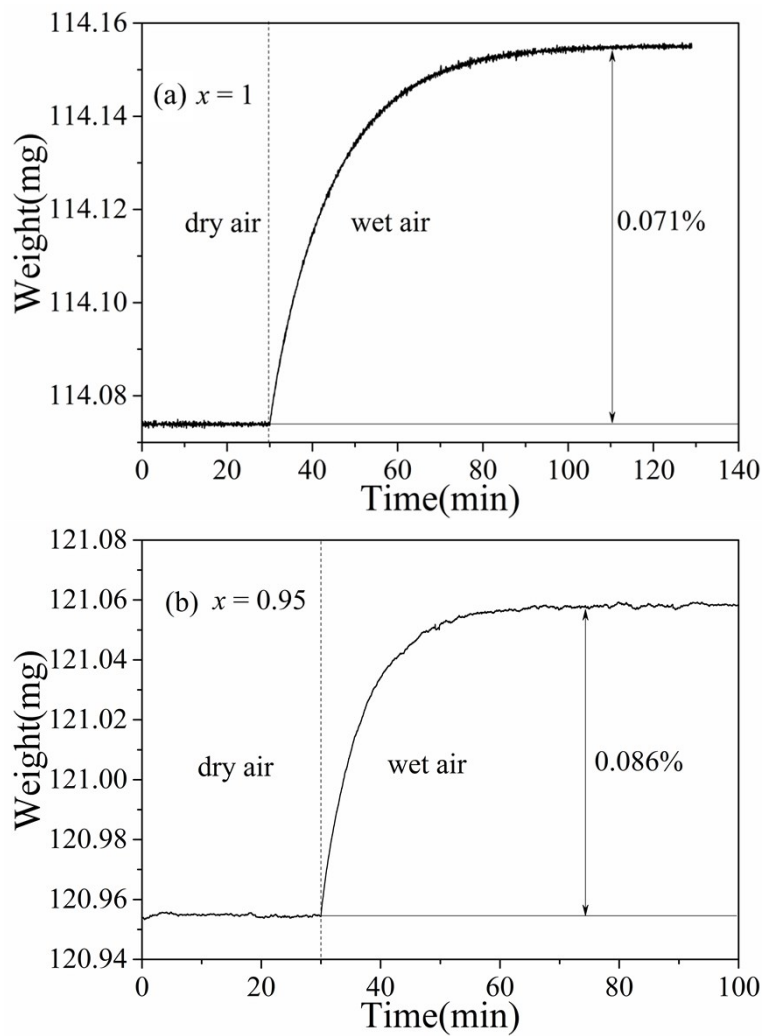


Fig. S8. Thermogravimetric relaxation curves for $\text{Ba}_x\text{Co}_{0.4}\text{Fe}_{0.4}\text{Zr}_{0.1}\text{Y}_{0.1}\text{O}_{3-\delta}$ pellet samples upon changing $p\text{H}_2\text{O}$ from dry condition to $p\text{H}_2\text{O} = 0.1\text{atm}$ at $500\text{ }^\circ\text{C}$. (a) $x = 1$ (b) $x = 0.95$.

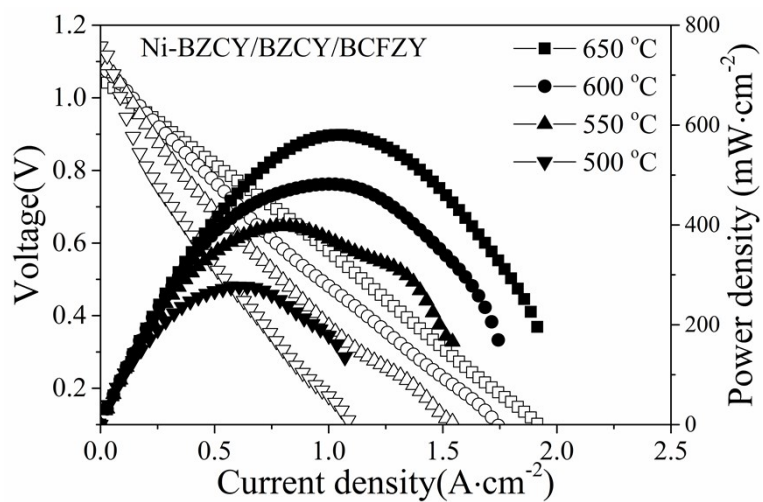


Fig. S9 Current-Voltage and Current-power density curves of cells based on BCFZY cathode operated from 650 to 500 °C, with humidified H_2 (3% H_2O) as anode fuel and ambient air as oxidant.